

An Inkjet-Printed Flexible Memristor Device for Echo State Networks

[†]Tasnim Zaman Adry, [†]Shahrin Akter, [†]Sazia Eliza, [‡]Steven D. Gardner, and [†]Mohammad Rafiqul Haider

[†]*Dept. of EECS, University of Missouri, Columbia, MO, U.S.A.*

[‡]*Dept. of ECE, University of Alabama at Birmingham, Birmingham, AL, U.S.A.*

{mhaider}@missouri.edu

Abstract—Neuromorphic computing, mimicking the neural structure of the brain, has made strides towards efficient data processing through the use of memristive devices, especially for sequential data challenges. In this innovative study, a cost-effective fabrication technique for flexible memristive devices utilizing inkjet printing technology is introduced. The devices feature the characteristic pinched hysteresis loop indicative of memristive behavior and are analyzed with a MATLAB empirical model, further visualized through a physical Simscape simulation. Leveraging these advancements, an Echo State Network with a memristor-based crossbar array is constructed, effectively demonstrating the practicality of Echo State Network deployment on flexible substrates with the potential to simplify training processes. This network, tested with a Mackey-Glass input, yields eight distinctive state vectors that serve as a foundation for signal output prediction. With a root-mean-square error of 2.4% in the initial reconstruction output, applying linear regression on the state vectors mirrors the functionality of an autoencoder, suggesting an inherent capability for feature extraction and dimensionality reduction. The resemblance to autoencoder behavior underscores the potential of the proposed system to refine signal reconstruction accuracy through unsupervised learning.

Index Terms—Neuromorphic computing, Memristors, Inkjet printing, MATLAB modeling, Echo State Network, Autoencoders

I. INTRODUCTION

Neuromorphic computing, inspired by the neural architecture of the human brain, represents a frontier in modern computational technology [1]. At its core, this approach seeks to transcend the limitations of traditional computing paradigms through the development of systems that mimic biological processes, enabling more efficient processing of complex, data-intensive tasks. Central to the realization of neuromorphic computing are memristive devices, components whose resistance varies according to the history of voltage and current that has been applied to them [2]. Memristors, first theorized by Leon Chua in 1971 and realized by HP Labs in 2008, are crucial for neuromorphic computing [3]. These devices offer a compact and energy-efficient means for advancing artificial neural networks [4], [5].

Among the various architectures proposed for neuromorphic computing, Echo State Networks (ESNs), a subset of recurrent neural networks (RNNs), are increasingly recognized for their straightforward design and effectiveness in managing sequential data [6]. These networks utilize a dynamic reservoir of neurons to process inputs in a way that reflects certain cognitive processing features of the brain [7], [8], making

them particularly adept at tasks like time-series prediction and pattern recognition—areas where traditional methods struggle with data complexity and timing issues. Recent advancements in neuromorphic computing have seen the development of memristor-based ESNs, which utilize the natural dynamics of memristive devices to emulate synaptic activity. Notable improvements in ESN performance and robustness have been achieved through new hardware designs by Hassan et al. [9], while Wang et al. have significantly enhanced energy efficiency and simplified training processes using a hardware-software co-designed echo state graph neural network [10]. The inherent structure and dynamics of ESNs also allow them to function effectively as autoencoders. Similar to how autoencoders compress data into a more compact form, ESNs can be trained to transform input data into the high-dimensional space of the reservoir to extract crucial features and subsequently learn to reduce these back to their original dimensionality or lower [11].

Despite the promise of echo state networks and memristive devices in advancing neuromorphic computing, these technologies' widespread adoption and implementation face significant challenges [12]. A primary obstacle is the fabrication of memristive devices, which often require complex, expensive processes that are not amenable to large-scale production or flexible computing applications. Addressing this challenge, our research introduces an innovative approach to constructing memristive devices using inkjet printing technology [13]–[18]. This method significantly reduces the cost and complexity associated with device fabrication and opens new avenues for integrating memristive devices into flexible electronic systems [19]. Recent studies have focused on developing novel materials, printing techniques, and device architectures for inkjet-printed memristors. Duraisamy et al. created a TiO_2 thin film memristor device using electrohydrodynamic inkjet printing, demonstrating bipolar resistive switching behavior at low voltages [20]. Bessonov et al. created memristive and memcapacitive switches with tunable resistance and low programming voltages using solution-processed $\text{MoO}_x/\text{MoS}_2$ and WO_x/WS_2 heterostructures [21]. Yoon et al. inducing memristor behavior in silver nanoparticle devices demonstrated controllable resistive switching behaviors for low-power flexible memory and synaptic learning applications [22]. The transition of memristors from theoretical to practical neuromorphic systems faces challenges like the absence of a

behavior-level simulator and reducing traditional fabrication techniques without compromising power efficiency.

This paper presents developing and characterizing an inkjet-printed flexible memristor device, demonstrating memristive behavior through its distinctive I-V curve. Simscape is used to build a physical model, while MATLAB's Curve Fitting tool (CFtool), is used to produce an empirical model. In this study, all simulations were carried out using MATLAB (version R2023b). The modeled memristor is integrated into a crossbar array structure to implement an ESN. The results show the potential of inkjet-printed memristive devices on flexible substrates for neuromorphic computing, reducing training complexity of ESNs. The network produces eight unique state vectors for predicting signal output, mimicking the operation of an autoencoder. The system's behavior is similar to autoencoders, demonstrating its ability to improve forecast accuracy through unsupervised learning. This approach demonstrates the feasibility of inkjet-printed memristive devices on flexible substrates for neuromorphic computing.

II. STRUCTURAL DESIGN AND FABRICATION

Using Matlab for numerical modeling, the study investigates the utilization of inkjet printing for the creation of an inexpensive, nonlinear, voltage-controlled graphene memristor device. Circuits that are inkjet printed (iJP) can be applied in nonuniform environments, like curved or uneven surfaces, textiles, and nonrigid objects. Fig. 1 depicts an iJP Memristor schematic. The memristor's development involved a trial and error approach, involving manual experimentation with various dimensions to ensure stability and manufacturability, with plans to refine them further.

The printing process involves assessing conductivity, aligning the gap with the print head's movement axis, and depositing silver plates spaced approximately $130\ \mu\text{m}$ apart. The channel area is then coated with hexagonal boron nitride (hBN) and cured at $150\ ^\circ\text{C}$ for five minutes to solidify it. This layer serves to insulate and manage the channel region. One challenge with iJP technology is the coffee-ring effect, which reduces the uniformity and reliability of the nanoparticle distribution. To counteract this, a novel approach has been developed where a well is created in the hBN layer to control the spreading and interaction of GN ink with the adjacent silver plates. This well can be created automatically using a V-One PCB printer. Finally, to mitigate the coffee-ring effect, the GN ink is carefully applied to the well.

III. I-V CHARACTERISTICS

The memristive behavior of the iJP memristor device—a memory effect that results in a loop rather than a single line on the I-V curve—was examined. Two great examples of hysteretic devices are Schmitt triggers and memristors, whose output signals can change into numerous states based on the signal's past. These devices are perfect candidates to be used as reservoirs because of their high non-linearity with varying states and natural time-series features. The hBN and GN/PEDOT: PSS mixture, which has a distinct I-V curve,

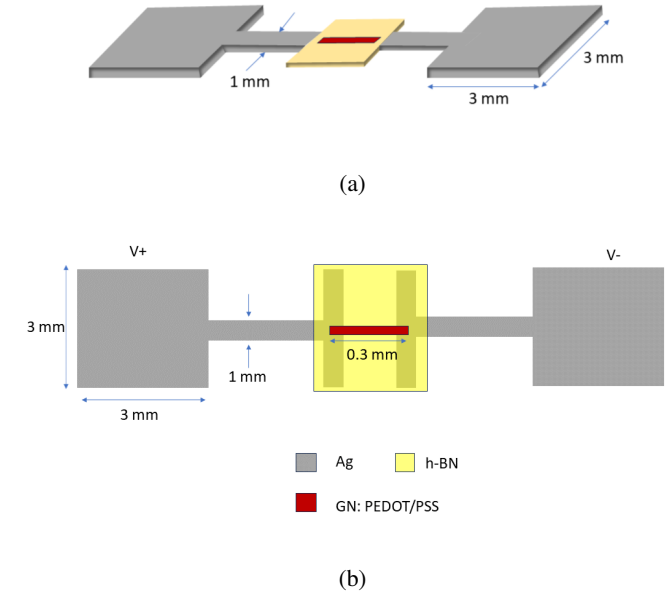


Fig. 1: Schematic of the memristor fabricated using inkjet printing. (a) A 3D view of the iJP memristor device; and (b) a top view of the device, complete with measurements.

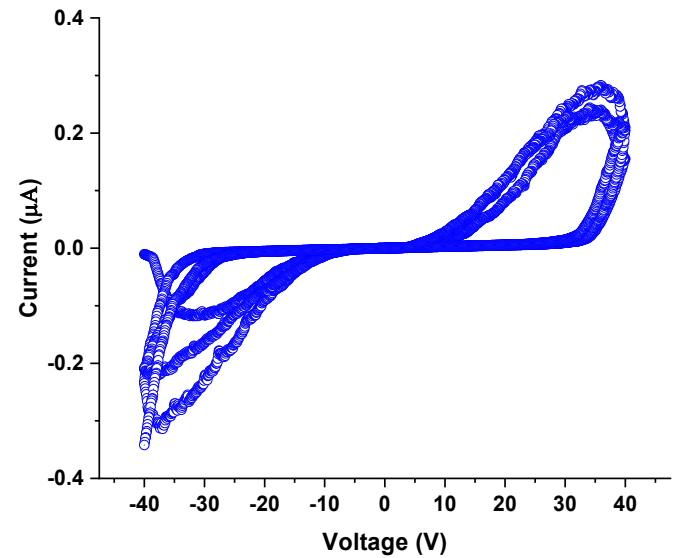


Fig. 2: Measured iJP memristor device's I-V characteristic. A complete pinched-hysteresis loop is seen.

was utilized as the semiconductor in the iJP memristors. The memristive activity of the device is accurately represented by the I-V curve of the iJP memristors, as illustrated in Fig. 2. The positive voltage steadily rises while the current abruptly jumps between 30 V and 40 V.

The device alternates between the low resistance state (LRS) and the high resistance state (HRS) throughout the SET process. It then returns to the LRS between -30 and 40 volts.

Due to complex exponential regressions, the signal is more challenging to simulate for simulation investigations. It displays noteworthy non-linearity and a characteristic hysteresis curve. This behavior is more linearly erratic than previous device results.

IV. MEMRISTOR MODELING IN MATLAB

The literature has reported on a number of memristor models. According to [23], the Ion-Drift model demonstrates no-threshold conduction. Yakopcic [24] reported a new model that exhibits a threshold in the forward pass but none in the backward pass. The designed iJP memristor displays thresholds in both forward and backward passes, in contrast to the other two methods. Therefore, in order to appropriately fit the experimental data, this study uses an empirical model created with MATLAB CFtool. The model creates separate equations for the forward (-40 V to 40 V) and backward (40 V to -40 V) runs of the I-V curve. After that, these equations are combined to create a 6th order polynomial that represents a perfect pinched hysteresis loop. The empirical equation looks like this:

$$y = p1 \cdot x^6 + p2 \cdot x^5 + p3 \cdot x^4 + p4 \cdot x^3 + p5 \cdot x^2 + p6 \cdot x + p7 \quad (1)$$

Table I provides specifics on how the variable values ($p1, p2, p3, p4, p5, p6, p7$) vary for forward and reverse passes. Fig. 3 displays the fitted curve and the experimental curve. Memristor behavior is replicated using empirical equations, demonstrating the usefulness of memristor modeling in MATLAB.

TABLE I: Parameters list

Parameters	Forward Pass	Backward Pass
$p1$	1.51×10^{-16}	-1.45×10^{-16}
$p2$	-1.04×10^{-15}	-1.02×10^{-15}
$p3$	-2.37×10^{-13}	1.82×10^{-13}
$p4$	4.7×10^{-12}	3.99×10^{-12}
$p5$	-3.57×10^{-11}	8.67×10^{-11}
$p6$	6.14×10^{-10}	1.43×10^{-9}
$p7$	1.51×10^{-10}	-1.43×10^{-10}

Exact simulation outcomes for input voltages ranging from -40 V to 40 V are depicted in Fig. 4. The simulation data, achieving an R^2 -value of 0.9972 in the forward direction and 0.9961 in the reverse, closely align with the experimental findings. It is advantageous to represent the memristor as an element within complex systems using a Simulink framework.

The Simulink environment includes the Simscape block library, intended for multidomain physical system modeling. We have created a physical Simscape model that may be applied to reservoir networks. Fig. 5 shows this model, where a Simscape script file containing the memristor model was used, and a Simscape component block was employed. Fig. 6 shows the output current of the Simulink model in response to a sinusoidal input voltage. As illustrated in Fig. 6, pinched hysteresis threshold voltages that arise during both forward and backward conduction processes cause the output current to be skewed.

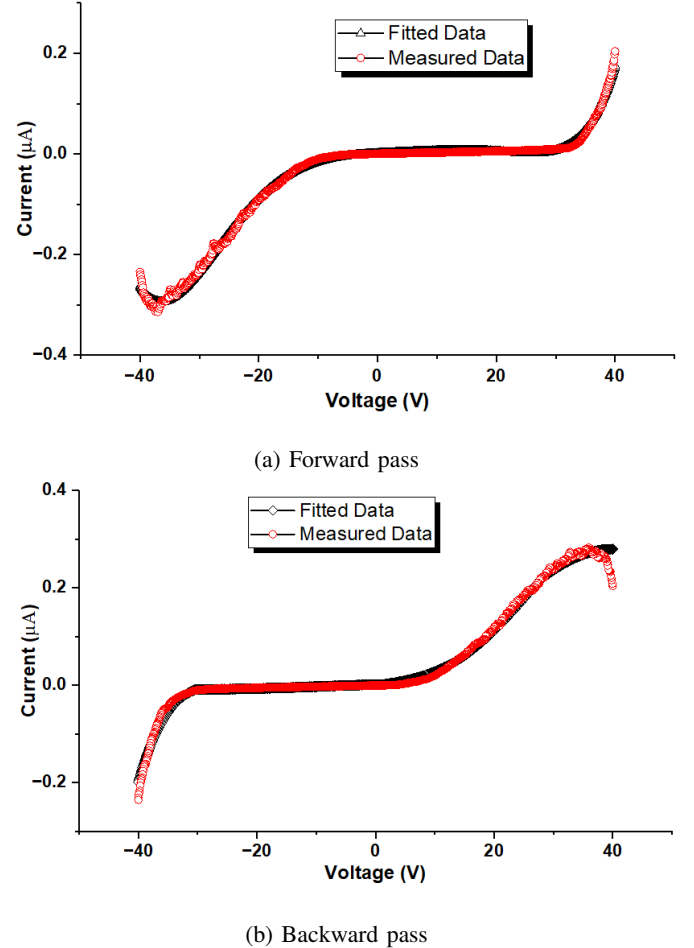


Fig. 3: Fitted curve to the measured data of the iJP memristor.

V. ECHO STATE NETWORK USING THE MEMRISTOR MODEL

Within the architecture of an ESN, memristors serve the role of synapses, forming connections between neurons. Arranged in a crossbar grid formation, these memristors provide tunable resistance levels — or memristance — corresponding to synaptic strength. This configuration permits the dynamic adaptation of synaptic weights, informed by previous signal activity, thereby augmenting the network's capacity for learning and processing temporal sequences.

For the construction of the ESN, we have seamlessly integrated our empirically derived model into a Simscape component, effectively transforming it into a dual-terminal device that serves as the fundamental building block of our network. Utilizing this building block, we assembled an 8 × 8 memristor crossbar array. Our ESN is designed with a reservoir comprising 144 neurons, strategically connected in a sparsely populated pattern to strike a delicate balance between the intricacies of network architecture and the practicality of computational efficiency, essential for processing data in real-time scenarios. The architecture of the memristor-based crossbar array, which forms the core of the ESN, is illustrated in

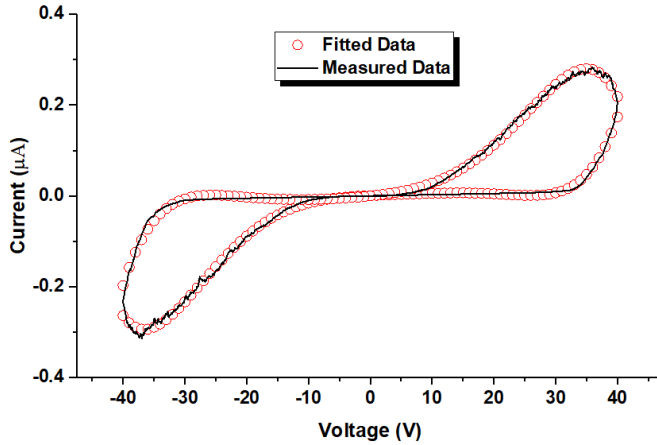


Fig. 4: Simulated I-V profile of the iJP memristor model showing pinched hysteresis.

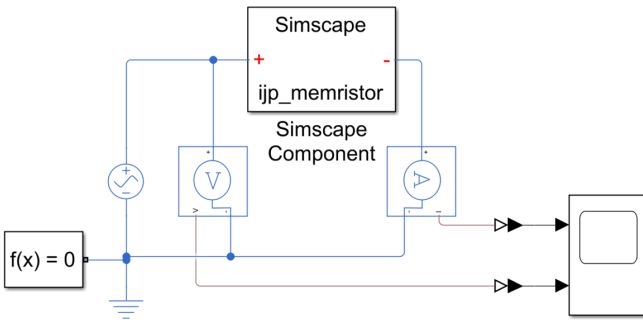


Fig. 5: Simscape model of the physical iJP memristor.

Figure 7. The study uses an 8x8 crossbar array for optimal complexity and performance in neuromorphic computing applications, with 144 neurons for robust pattern recognition and input signal prediction or autoencoding application.

For the input, we employed the Mackey-Glass signal, a common choice in time series prediction and chaotic system analysis, and a standard in training and testing neural networks like Echo State Networks (ESNs). Outputs were sampled from various nodes within the network, as depicted in Figure 8, which illustrates the input and output states of the ESN.

The state vectors generated by the ESN were utilized in a linear regression model to reconstruct the input signal. The model achieved an impressive Root Mean Square Error (RMSE) of 2.4%, demonstrating an autoencoding functionality. This indicates the potential of the proposed ESN to function as a Vanilla autoencoder. Within the ESN framework, by fine-tuning the readout weights, the network can effectively learn to encode significant features from inputs into the reservoir. These features are then decoded to regenerate the input, mirroring the function of the hidden layer in a traditional autoencoder. Figure 9 shows the input signal and the reconstructed signal through the ESN.

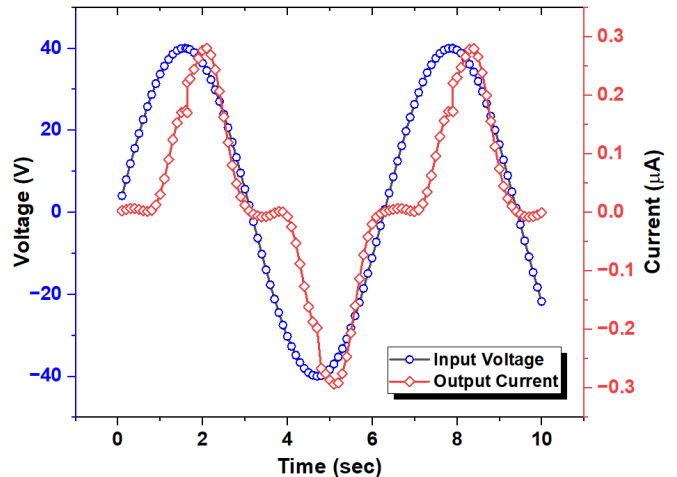


Fig. 6: Time response of the iJP memristor showing the input sinusoidal voltage and the corresponding skewed output current due to the pinched hysteresis behaviour of the device.

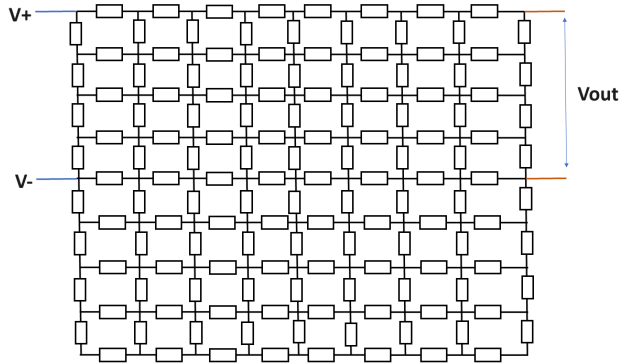


Fig. 7: The iJP memristor based crossbar array as a reservoir for the ESN.

VI. CONCLUSION

This research represents a notable breakthrough in developing flexible, affordable memristive devices utilizing inkjet printing technology, a step in line with the escalating demand for scalable neuromorphic computing systems. By successfully demonstrating the production of memristive devices on flexible substrates, we address significant challenges in cost and adaptability for neuromorphic applications. The inkjet-printed memristors featured in this study display characteristic pinched hysteresis loops, a definitive sign of genuine memristive behavior essential for the effective operation of ESNs. Both empirical and physical modeling, particularly using MATLAB and Simscape, confirm these devices' capabilities in simulating synaptic activities crucial to neuromorphic computing. Integrating these memristors into a crossbar array structure for ESNs is anticipated to reduce training complexity and enhance computational efficiency, potentially paving the way toward more energy-efficient, high-performance neuromorphic systems. Furthermore, this ESN demonstrates potential as a

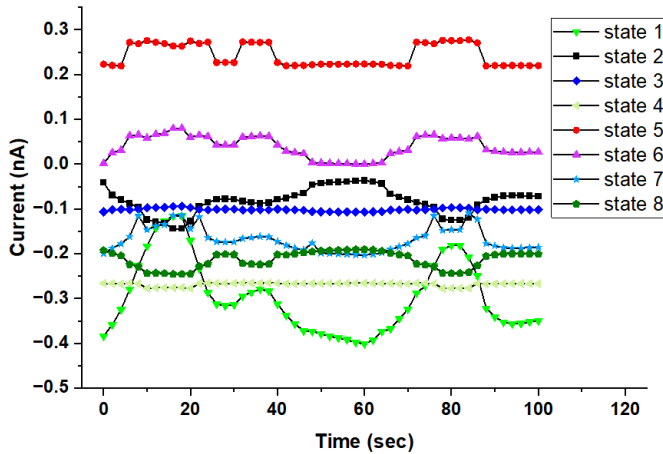


Fig. 8: The output state vectors of the Mackey-Glass signal from the iJP memristor based ESN.

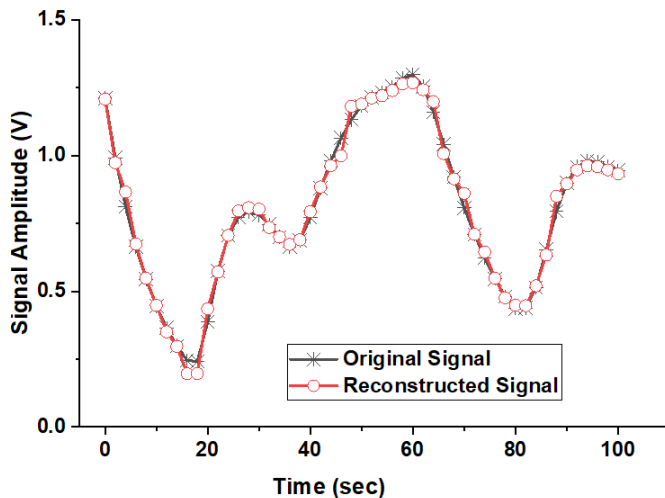


Fig. 9: The reconstructed Mackey-Glass signal using the state vectors from the iJP memristor based ESN.

Vanilla autoencoder. This study contributes significantly to the overarching aim of developing scalable, cost-effective neuromorphic systems capable of processing data-intensive operations with exceptional energy efficiency, marking a critical advancement in computing technology evolution.

ACKNOWLEDGMENT

This work was supported by the USA National Science Foundation (NSF) under Grant No. ECCS-2201447. Any opinions, findings, conclusions, or recommendations expressed in this material are those of the author(s) and do not necessarily reflect the views of the National Science Foundation.

REFERENCES

- [1] K. Roy, A. Jaiswal, and P. Panda, "Towards spike-based machine intelligence with neuromorphic computing", *Nature*, vol. 575 no. 7784, pp. 607-617, 2019.
- [2] J. Del Valle, et al., "Challenges in materials and devices for resistive-switching-based neuromorphic computing", *Journal of Applied Physics*, vol. 124, no. 21, 2018.
- [3] L. Chua, "Memristor-the missing circuit element", *IEEE Transactions on circuit theory*, vol. 18, no. 5, pp.507-519, 1971.
- [4] K. Sun, J. Chen, and X. Yan, "The future of memristors: Materials engineering and neural networks", *Advanced Functional Materials*, vol. 31, no. 8, pp. 2006773, 2021.
- [5] H. Jeong, and L. Shi, "Memristor devices for neural networks", *Journal of Physics D: Applied Physics*, vol. 52, no. 2, pp. 023003, 2018.
- [6] S. D. Gardner, M. R. Haider, L. Moradi and V. Vantsevich, "A Modified Echo State Network for Time Independent Image Classification," *2021 IEEE International Midwest Symposium on Circuits and Systems (MWSCAS)*, Lansing, MI, USA, 2021, pp. 255-258.
- [7] G. Tanaka, et al., "Recent advances in physical reservoir computing: A review", *Neural Networks*, vol. 115, pp. 100-123, 2019.
- [8] H. Jaeger, "The 'echo state' approach to analysing and training recurrent neural networks-with an erratum note", *German Nat. Res. Center Inf. Technol., Bonn, Germany, GMD Report*, vol. 148, p. 13, 2001.
- [9] A. M. Hassan et al., "Hardware implementation of echo state networks using memristor double crossbar arrays", in *2017 International Joint Conference on Neural Networks (IJCNN)*. IEEE, 2017.
- [10] S. Wang, et al., "Echo state graph neural networks with analogue random resistive memory arrays", *Nature Machine Intelligence*, vol. 5, no. 2, pp. 104-113, 2023.
- [11] H. Wang, et al., "Optimizing deep belief echo state network with a sensitivity analysis input scaling auto-encoder algorithm", *Knowledge-Based Systems*, vol. 191, pp. 105257, 2020.
- [12] S. Wen, et al., "Memristor-based echo state network with online least mean square", *IEEE Transactions on Systems, Man, and Cybernetics: Systems*, vol. 49, no. 9, pp. 1787-1796, 2018.
- [13] R. Lu, M. R. Haider, S. Gardner, J. I. D. Alexander and Y. Massoud, "A Paper-Based Inkjet-Printed Graphene Sensor for Breathing-Flow Monitoring," in *IEEE Sensors Letters*, vol. 3, no. 2, pp. 1-4, Feb. 2019, Art no. 6000104.
- [14] S. D. Gardner, J. I. D. Alexander, Y. Massoud and M. R. Haider, "An Inkjet-Printed Paper-Based Flexible Sensor for Pressure Mapping Applications," *2020 IEEE International Symposium on Circuits and Systems (ISCAS)*, Seville, Spain, 2020, pp. 1-5.
- [15] S. D. Gardner, M. R. Opu and M. R. Haider, "An Inkjet-Printed Capacitive Sensor for Ultra-Low-Power Proximity and Vibration Detection," *2023 IEEE Wireless and Microwave Technology Conference (WAMICON)*, Melbourne, FL, USA, 2023, pp. 73-76.
- [16] S. D. Gardner, J. I. D. Alexander, Y. Massoud, and M. R. Haider, "Minimally produced inkjet-printed tactile sensor model for improved data reliability," *2020 11th International Conference on Electrical and Computer Engineering (ICECE)*, Dhaka, Bangladesh, 2020, pp. 49-52.
- [17] M. R. Opu, S. D. Gardner and M. R. Haider, "A Low-Cost Inkjet-Printed Hear Sound Sensor for Telehealth Application," *2023 IEEE 66th International Midwest Symposium on Circuits and Systems (MWSCAS)*, Tempe, AZ, USA, 2023, pp. 197-201.
- [18] S. D. Gardner, and M.R. Haider, "An inkjet-printed artificial neuron for physical reservoir computing", *IEEE Journal on Flexible Electronics*, vol. 1, no. 3, pp. 185-193, 2022.
- [19] S. D. Gardner, M. R. Haider, M. T. Islam, J. I. D. Alexander and Y. Massoud, "Aluminum-doped Zinc Oxide (ZnO) Inkjet-Printed Piezoelectric Array for Pressure Gradient Mapping," *2019 IEEE 62nd International Midwest Symposium on Circuits and Systems (MWSCAS)*, Dallas, TX, USA, 2019, pp. 1101-1104.
- [20] N. Duraisamy et al., "Fabrication of TiO₂ thin film memristor device using electrohydrodynamic inkjet printing", *Thin Solid Films*, vol. 520, no. 15, pp. 5070-5074, 2012.
- [21] A. A. Bessonov et al., "Layered memristive and memcapacitive switches for printable electronics", *Nature materials*, vol. 14, no. 2, pp. 199-204, 2015.
- [22] K.J. Yoon, et al., "Electrically-generated memristor based on inkjet printed silver nanoparticles", *Nanoscale Advances*, vol. 1, no. 8, pp. 2990-2998, 2019.
- [23] S. Kim, S. Choi, and W. Lu, "Comprehensive physical model of dynamic resistive switching in an oxide memristor", *ACS nano*, vol. 8, no. 3, pp. 2369-2376, 2014.
- [24] C. Yakopcic et al., "Memristor model optimization based on parameter extraction from device characterization data", *IEEE Transactions on Computer-Aided Design of Integrated Circuits and Systems*, vol. 39, no. 5, pp. 1084-1095, 2019.